Seismic rehabilitation of cultural heritage masonry buildings with unbonded fiber reinforced elastomeric isolators (U-FREIs) – A case of study

Journal of Cultural Heritage xxx (2017) xxx–xxx

Available online at
ScienceDirect
www.sciencedirect.com

Elsevier Masson France
EM|consulte
www.em-consulte.com/en

Original article

Seismic rehabilitation of cultural heritage masonry buildings with unbonded fiber reinforced elastomeric isolators (U-FREIs) – A case of study

Margherita Pauletta*, Daniele Di Luca , Eleonora Russo , Cristina Fumo

Polytechnic Department of Engineering and Architecture, University of Udine, Viale delle Scienze 206, 33100 Udine, Italy

ARTICLE INFO

Article history:
Received 13 April 2017
Accepted 22 September 2017
Available online xxx

Keywords:
Masonry
Historical building
Unbonded fiber reinforced elastomeric isolator
Non-linear analysis
Seismic rehabilitation

ABSTRACT

In order to assess the structural behavior and to evaluate the seismic vulnerability of masonry structures of relevant historical and artistic significance, which is a widespread building type in Italy and in the world, an historical masonry church is analyzed under earthquake loading. Linear and non-linear analyses are performed on the finite element models of the structure. From these analyses it is pointed out that the structure does not behave elastically in its existing condition even when subjected to the frequent design earthquake (81% probability of being exceeded over 50 years). Two traditional rehabilitation methods are studied: the placement of a rigid diaphragm which connects the top of the masonry walls only enclosing the church entrance area and the placement of a rigid diaphragm which connects the tops of all masonry walls. None of the traditional method is sufficient for the structure to survive basic design earthquake (10% probability of being exceeded over 50 years). Hence an advanced seismic retrofit solution using innovative carbon fiber reinforced elastomeric isolators is proposed. The proposed intervention consists in the installation of six Unbonded Fiber-Reinforced Elastomeric Isolators (U-FREI) and six Flat Surface Sliders (FSS) as passive protective devices besides the placement of a rigid diaphragm which connects the tops of all masonry walls. The process of installation of the devices is illustrated. The use of the proposed solution leads to a remarkable enhancement of the seismic response capacities of the structure; indeed a general elastic response under the Basic Design Earthquake (BDE) is attained.

1. Introduction

A great number of the historical or culturally significant monuments in Italy are church masonry buildings. These historical buildings are generally able to safely carry the vertical loads, but they are particularly susceptible to damage, and prone to partial or total collapse under earthquake horizontal loads, sometimes in the presence of ineffective restoration [1].

The seismic vulnerability of this type of building is due to both the configuration, often characterized by open spaces, façades sparingly interconnected with the perpendicular walls, flexible wooden roofs, and the mechanical properties of the masonry material, which has highly nonlinear behavior and very low tensile strength [2].

Impediments to and restrictions on inspection of historic construction, or difficulties with the removal of specimens in buildings of historical value, as well as the high costs involved in inspection and diagnosis, often result in limited information about the internal constructive system or the properties of existing materials.

Moreover, it must be stressed that the structural resistance of material decreases over time due to deterioration, and this degradation is frequently accelerated by lack of maintenance or carelessness [1].

Because of the uncertainties that affect the structural behavior and mechanical properties, it is difficult to reduce historical buildings to any standard structural scheme. The above considerations explain the need of specific modeling and analysis strategies for such constructions.

One of the criteria used to classify the structural modelling techniques in general and for historical masonry structures too is the complexity of the mathematical models adopted to describe the materials behavior. A simple wide-spread method is the "limit analysis" [3], which requires an a priori detection of potential crisis mechanisms.

* Corresponding author.
E-mail addresses: margherita.pauletta@uniud.it (M. Pauletta), diluca.daniele@spes.uniud.it (D. Di Luca), russoeleonora@hotmail.com (E. Russo), cristina.fumo@uniud.it (C. Fumo).

https://doi.org/10.1016/j.culher.2017.09.015
1296-2074/

Thanks to the availability of more powerful computing tools, more refined structural models have emerged in recent years, and the non-linear finite elements approach has become a popular analysis technique. Detailed investigations about masonry modelling techniques are provided in [4], while reviews on constitutive laws used to model the brittle behavior of masonry structures is provided in [5] and [6].

In accordance with the classification formulated in [7] it is possible to distinguish two main finite-elements modelling approaches: macro-models and micro-models.

In macro models [6] and [8–13] the masonry, usually made of brick elements and mortar joints, is simulated as isotropic or anisotropic homogenous material with equivalent mechanical properties. The main problem in this compound is to define representative mechanical properties of the masonry, since it is well known that brick elements and mortar joints have different stress-strain properties under normal and shear stresses.

In micro models [14–17] the spatial discretization of the masonry is reduced to the simulation of brick elements and mortar joints. Micro models use contact elements to model the connection between the brick elements and mortar joints. This approach provides a more realistic representation of the masonry behavior, because it is able to describe local effects in each material and at their contact, but it demands a great number of relatively small finite elements and contact elements, i.e. a greater computational cost.

In the numerical simulation of masonry structures by the Finite Element Method (FEM), different tendencies were developed to represent the cracks. The discrete crack models are based on the idea of always working with the portion of the solid which remains continuous and without any damage, so that during the formation or progression of an existing crack, its sides incorporate to the outline of the solid. The cracks are modelled as displacement discontinuities among the finite elements and they must develop across their outlines, what ends up generating a restriction in its propagation direction. In the smeared crack models, otherwise, the cracked material is treated as continuous, and the discontinuity of the displacement field caused by the crack is spread across the element by changing the constitutive equation instead of changes on the finite element mesh [18]. The smeared crack models permit to simulate the post-crack behavior of the material allowing to follow up the evolution of stresses and strains during the loading process and to obtain a crack pattern which enabled to better understand its behavior, as well as to follow up the stress evolutions [18].

A seismic analysis of an historical building, whose model is entirely constituted of smeared cracking elements, is presented herein. The main references for the used smeared crack model are [2], and [1,19,20]. The described case concerns the seventeenth-century private church known as Lippomano Villa Oratory (Figs. 1-2), located in the Monticella hill, district within the municipality of Conegliano, about 70 m a.s.l. and 30 km north of Treviso, Italy. The church structural behavior with respect to

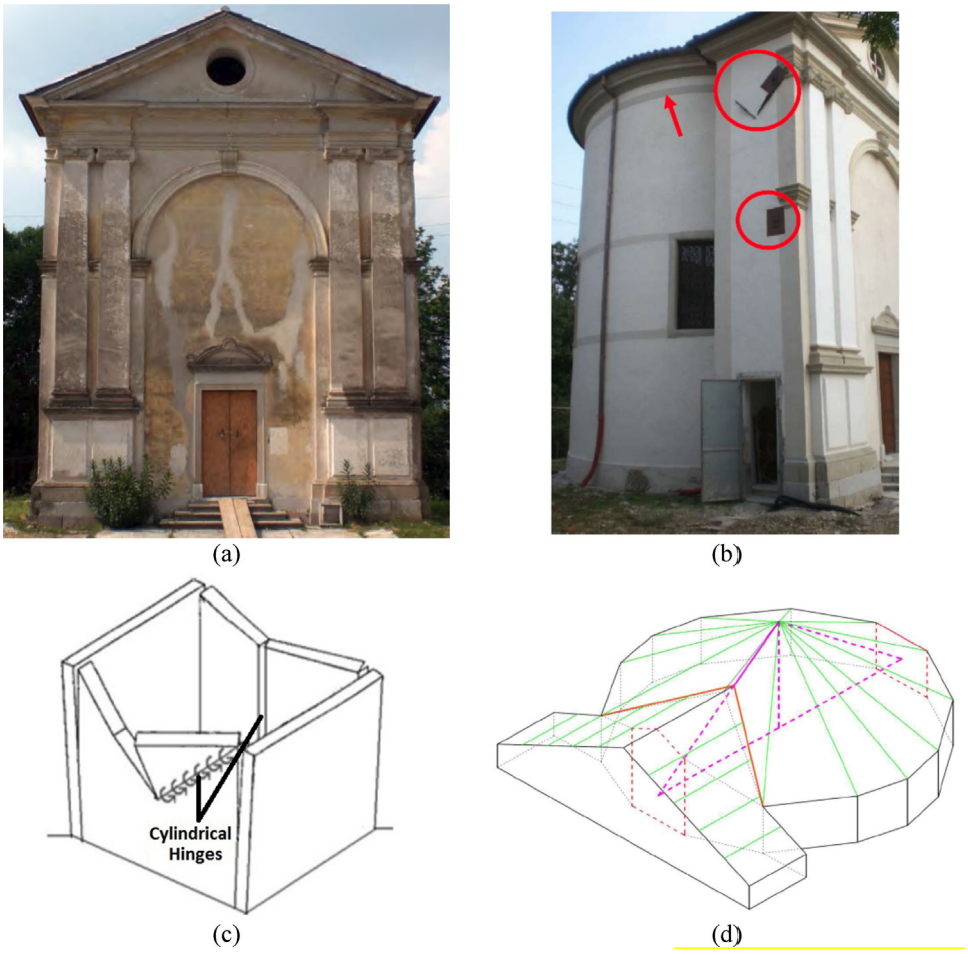

Fig. 1. Lippomano Villa Oratory: (a) main entrance on the south side after architectural restoration [21]; (b) south-west side after restoration with the anchoring ties highlighted by the circles and reinforcing ring indicated by arrow [21]; (c) typical out-of-plane collapse mechanism of masonry buildings; (d) simplified structural scheme of the wooden roof.

Please cite this article in press as: M. Pauletta, et al., Seismic rehabilitation of cultural heritage masonry buildings with unbonded fiber reinforced elastomeric isolators (U-FREIs) – A case of study, Journal of Cultural Heritage (2017), https://doi.org/10.1016/j.culher.2017.09.015

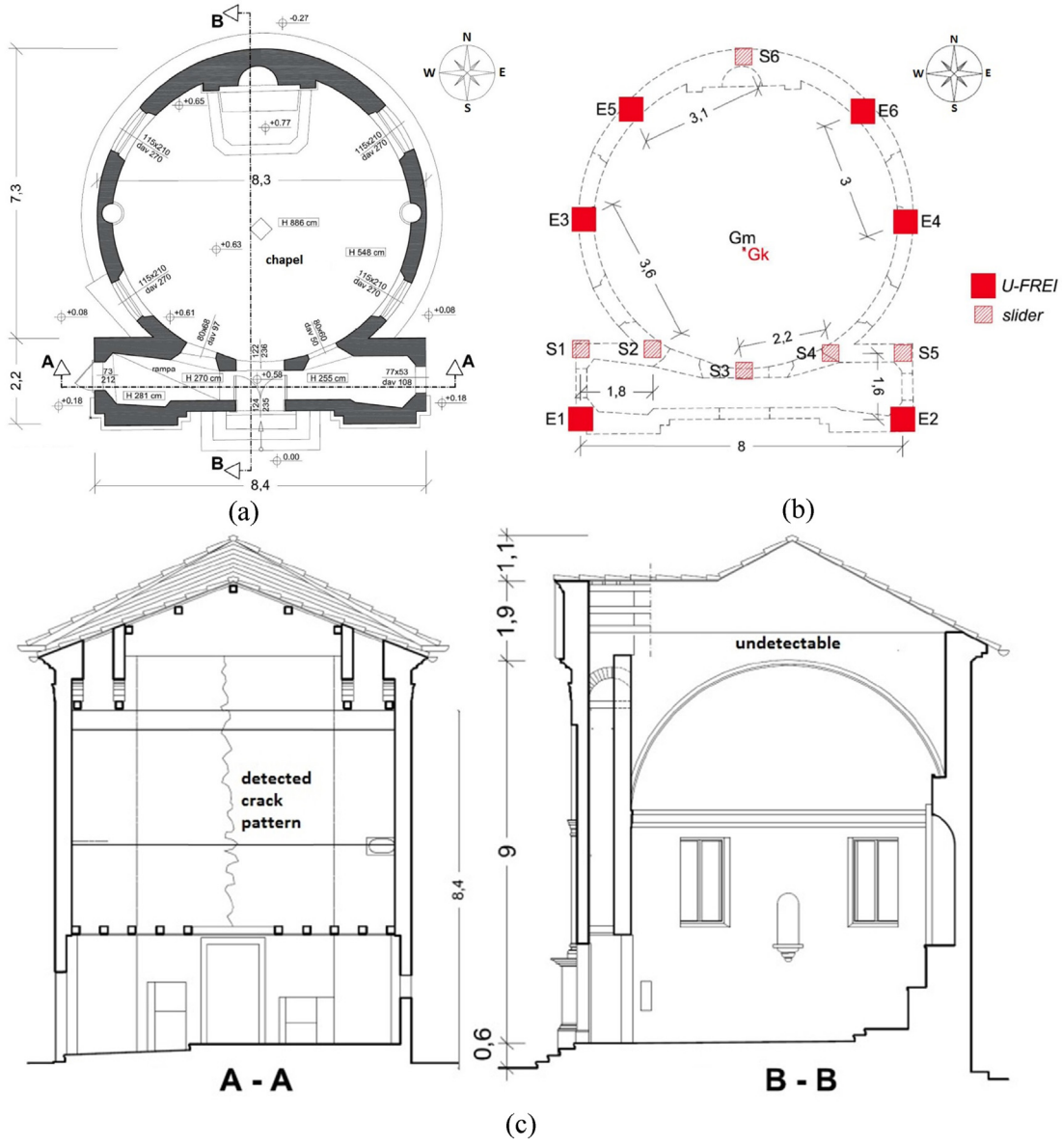

Fig. 2. Lippomano Villa Oratory: (a) ground floor plan; (b) designed isolation system; (c) sections A-A and B-B [21].

the actual state of conservation is investigated, and an innovative rehabilitation intervention is proposed.

2. Research significance

The aim of the present study is to show the efficiency of an advanced seismic retrofit solution, consisting of the installation of innovative unbonded fiber-reinforced elastomeric isolators, to achieve adequate protection levels for historic masonry buildings.

3. Case study

3.1. Existing condition

The Lippomano Villa Oratory (Fig. 1) is an historical brick masonry structure, part of the Italian artistic and cultural heritage. Geometrically, it is constituted of the union of two volumes (Fig. 2(a)). The first volume contains the main entrance area, having the dimensions of 8.4 m long and 2.2 m wide; the height of the façade is about 11 m, and it is topped by a wooden saddle roof. The second volume contains the main room, i.e. the chapel; it has a barrel shape with a diameter of about 8.3 m and cone-shaped wooden roof (Fig. 2). The roof is supported by the top of the chapel barrel walls at a height of 9.6 m and has a height of 3.0 m. Its structural scheme, unknown because it is hidden by a ceiling system (Fig. 2(c)), is deduced through comparison with roofs of similar churches built in the area during the same historical period (Fig. 1(d)).

The walls' thickness ranges between 0.4 m and 0.8 m.

No information is available about the foundations, which are presumed to be the simple continuation of the masonry walls.

In the recent past, the church was strengthened by means of anchoring ties to improve the connection between east and west walls of the entrance hall, and a reinforcing ring made by a steel plate installed at the base of the cone-shaped wooden roof. Even more recently the plaster was renewed (Fig. 1(b)), hiding a critical crack pattern, evident from the photo in Fig. 1(a), that can be traced back to the incipient formation of a typical out-of-plane collapse mechanism of the church south façade (Fig. 1(c)). This mechanism

Please cite this article in press as: M. Pauletta, et al., Seismic rehabilitation of cultural heritage masonry buildings with unbonded fiber reinforced elastomeric isolators (U-FREIs) – A case of study, Journal of Cultural Heritage (2017), https://doi.org/10.1016/j.culher.2017.09.015

is due to the slenderness of the façade and to the absence of a structural system connecting the tops of the walls at the base of the roof and will be described well in the following.

4. Analysis method

At present, the most widely adopted approach in analyzing existing masonry buildings, as recommended by Italian Guidelines for Cultural Heritage [22], presumes, or pre-assigns, a failure mechanism based on a collection of most probable partial failure mechanisms. These include out-of-plane façade overturning, bell-tower collapse, apse shear, rocking failure, and other phenomena commonly observed in earthquake surveys. In the Italian Guidelines approach, the collapse multiplier of an unreinforced masonry frame is evaluated by applying the kinematic theorem of limit analysis for no-tension materials. The most vulnerable damage mechanisms are considered to be the failure mechanisms linked to the lower value of the collapse multiplier that coincides with the non-dimensional horizontal acceleration at collapse.

The Italian guidelines approach, while straightforward and easily applied, has two noteworthy drawbacks [2]. First, there is a risk of overestimating the horizontal acceleration at failure. The upper-bound theorem of limit analysis states that the actual mode of collapse corresponds to the smallest kinematically admissible multiplier. Therefore, if the actual failure mechanisms that determine the vulnerabilities are different from those presumed in accordance with the Italian Guidelines, an overestimation of the collapse multipliers occurs. Second, the approach does not take into account the fact that masonry exhibits several characteristics that may play an important role in the formation of the failure patterns. For example, the orthotropic nature of masonry cannot be described by the utilization of a no-tension material model. Furthermore, in reality, the texture of the brickwork considerably influences what the model assumes to be monolithic behavior against out-of-plane loads.

Refined mechanical models, which accurately predict the behavior of masonry material and elements, have been proposed in the literature [23–28]. Such models adopt different strategies to take into account the highly non-linear behavior of the material both in tension (low tensile capacity and consequent cracking phenomena) and in compression. Some of the models are also able to provide the structural response to large cyclic deformations, which occur under seismic actions. Unfortunately, they are hardly applicable to the complete 3D analysis of complex structural systems, due to the great number of parameters involved in the definition and updating of the mechanical model, and the large number of degrees of freedom required for structural meshing, conditions which lead to untreatable problems [1].

In this paper fundamental dynamic properties of the case study are worked out by using the finite element method. Dynamic linear and nonlinear analyses are performed on 3D models of the church. For the linear analysis, the standard FEM modeling strategy based on the concepts of homogenized material and elastic constitutive laws is used, while, for the non-linear analysis, the behavior of the masonry is modeled with solid elements, whose stiffness is modified by the development of cracking and crushing, according to the chosen smeared cracking constitutive law.

The internal stress distribution of the church masonry structure obtained from the linear elastic model and the non-linear one are compared up to the instant at which, as consequence of significant structural damage, the results of the non-linear model diverge significantly from the results of the linear one. The purpose is to identify the stress pattern that gives origin to cracking in the masonry walls, which anticipates the development of failure mechanisms.

In this way, linear dynamic analysis results are used to assess whether the structure is able to ensure a general elastic response (i.e. no damage) during the whole seismic event.

5. Finite element models

Dynamic time-history analyses are carried out on the 3D models of the church structural complex using the Finite Element codes SAP2000 for the linear elastic analysis and Fast Non-linear Analysis [29] (FNA) and ANSYS Mechanical APDL, for the non-linear elastic one.

ANSYS, allowing the modeling of masonry non-linearity, is used to study the non-linear behavior of the fixed-base configuration of the building, to distinguish the main and most dangerous damage patterns, whose development may give rise to the formation of collapse mechanisms. As regards the isolation system proposed in this research, in order to achieve the best plan configuration for the isolators, numerous non-linear time-history analyses are required, which generally involve long computation time if non-linearity is diffused as in the ANSYS model.

On the other hand SAP2000, which provides only a linear constitutive relationship for masonry, allows describing the overall dynamic behavior of the structure through FNA method which involves nonlinearities concentrated only in the non-linear links, i.e. the isolators. Thanks to this method the computational cost is reduced and a greater number of nonlinear analyses to determine the ideal number and positioning of the base isolation devices is allowed.

In this study a correspondence between the “first damage state” found by ANSYS and the corresponding stress distribution in SAP2000 is searched. This stress distribution is then considered as the one involving failure of the structure and SAP2000 is used for subsequent analyses because of the lower computational cost required.

The masonry linear behavior is modeled in SAP2000 through thick-shell elements [30]. A Mindlin-Reissner formulation is used to model the plate behavior.

The masonry non-linear behavior is represented in ANSYS by combining plastic behavior with the chosen smeared crack approach. To reach this goal, the masonry walls are modeled by means of SOLID65 tetrahedral elements [31], which are defined by eight nodes and isotropic material properties.

In order to reduce the number of parameters involved in the definition of the masonry non-linear behavior, a Drucker-Prager perfectly plastic criterion [32] is employed, avoiding the need for definition of a hardening rule [1]. To define the yield surface, a non-associated flow rule is assumed; therefore cohesion c, internal friction angle ϕ and dilation angle ϕ_{dil} are the only material parameters required.

The masonry failure is predicted through the Willam-Warnke yield criterion [33]. Despite the need for five constants in order to define the criterion, in most practical cases [1] the adopted failure surface is defined by only the uniaxial tensile strength ft and the uniaxial compressive strength fc, since a proper selection of these values is adequate to cut off the tensile strength and to set an upper limit to the biaxial compressive strength [34]. The cross section of the assumed failure surface is defined by a cyclic symmetry about each 120° sector of the deviatoric plane. Both cracking and crushing failure modes are accounted for. The presence of a crack at each integration point is represented through modification of the stress-strain relationships by introducing a plane of weakness in a direction normal to the crack face. Also, shear transfer coefficients are introduced depending on the crack status, βt for open, or βc for re-closed, representing reduction factors for shear strength of

Please cite this article in press as: M. Pauletta, et al., Seismic rehabilitation of cultural heritage masonry buildings with unbonded fiber reinforced elastomeric isolators (U-FREIs) – A case of study, Journal of Cultural Heritage (2017), https://doi.org/10.1016/j.culher.2017.09.015

cracks subjected to shear stresses in the stages of opening and closing, respectively.

The non-linear model previously described, combining Drucker-Prager and Willam-Warnke criteria, effectively approximates the small tensile strength of the masonry, the plasticity behavior in the regime of average compression values, and the crushing phenomenon for high compressive stress.

Hook NLLink element in SAP2000 and Link180 element in ANSYS MAPDL are used to model the non-linear behavior of the steel anchoring ties connecting the east and west walls of the church entrance.

The flexible wooden roof is considered only in terms of seismic masses, and the relevant forces are assigned to the tops of the masonry walls that support them; thus the roof structure is not modeled.

Values that define the physical properties of masonry material were estimated using code prescriptions [35] and considering the conservative assumptions made by other authors who performed similar modeling of analogous buildings [1,2,36,37]. In particular, the masonry Young's modulus E is taken equal to 1500 MPa, Poisson modulus ν equal to 0.20, own weight γ equal to 1800 kg/m^3, cohesion c equal to 0.09 MPa, friction angle ϕ equal to 38°, dilation angle ϕdil equal to 15°, uniaxial tensile strength ft equal to 0.10 MPa, uniaxial compressive strength fc equal to 3.20 MPa, shear transfer coefficient for open cracks βt equal to 0.15, shear transfer coefficient for closed cracks βc equal to 0.75.

Preliminary modal analyses were performed to assess the agreement in results of the analyses obtained with the two finite element Codes, ANSYS and SAP2000. The fundamental frequency of the structure obtained from the model realized by ANSYS was equal to 2.91 Hz (period = 0.34 s) and involved a participating mass of 14.8% in the north-south direction (Fig. 2(a)). The corresponding mode involved the out of plane vibration of the south façade upper middle part.

The fundamental frequency of the structure obtained from the model realized by SAP2000 was equal to 2.8 Hz (period = 0.36 s) and involved a participating mass of 15.9% in the north-south direction. Also in this case the corresponding mode involved the out of plane vibration of the south façade upper middle part.

On the basis of these values it can be said that the results obtained by the two software are in good agreement.

6. Input earthquakes

The performance assessment of the structure's seismic behavior is carried out through incremental dynamic analyses, which are performed starting from the four reference seismic levels (limit states) set by standards [35], namely: the Frequent Design Earthquake (FDE), with an 81% probability of being exceeded over the reference time period VR; the Serviceability Design Earthquake (SDE), with a 50%/V_R probability; the Basic Design Earthquake (BDE), with a 10%/V_R probability; and the Maximum Considered Earthquake (MCE), with a 5%/V_R probability. The V_R period is fixed at 50 years, as obtained by multiplying the nominal structural life V_N of 50 years by an utilization factor equal to 1 assumed for buildings not subject to crowding, which applies to the Lippomano private church.

By referring to the topographic category T1 (flat surface), and C-type soil (deep deposits of dense or medium-dense sand, gravel or stiff clay from several ten to several hundred meters thick) according to code prescription [35], the peak ground accelerations (PGA) for the four seismic levels specified above result as follows: 0.058 g (FDE), 0.079 g (SDE), 0.228 g (BDE), and 0.309 g (MCE), where g is the gravity acceleration. Three artificial accelerograms generated from each of the four elastic pseudo-acceleration response spectra

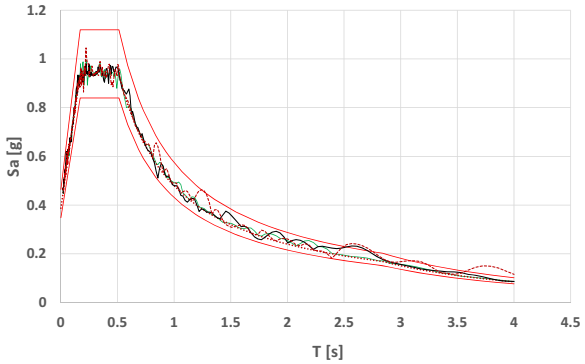

Fig. 3. The three accelerograms generated for the MCE compared to the design response spectrum.

associated to these peak ground accelerations are used as inputs to the non-linear dynamic analyses. Three groups of accelerograms are applied to the building for each limit state. For each group, the same accelerogram is contemporarily applied in both main horizontal directions of the structure, i.e. north-south and east-west (for the directions see plan in Fig. 2). The three accelerograms generated for the MCE are compared to the design response spectrum in Fig. 3, where the dotted regular line represents the response spectrum, the irregular lines the accelerograms and the continuous regular line the boundaries of the compatibility area inside which the accelerogram has to lay.

Actions and displacements of the structure are elaborated taking the most unfavorable values obtained from the analyses, as provided by the Code [35] when less than seven groups of accelerograms are used for a limit state.

7. Traditional rehabilitation interventions

The goal of rehabilitation of masonry structures, especially in seismically active areas, is typically to make them behave like a rigid block, with stiff floors and effective connections between the walls. However, for historic buildings in particular, such attempts must be made while striving for non-invasiveness; that is, removability of the interventions and compatibility of materials and construction techniques. In order to respect the existing features of the considered constructions, special care must be taken to limit variations in the external appearance and, if possible, to minimize variations in the original structural scheme. Rehabilitation efforts must respond to these conservative design criteria while ensuring that the proposed interventions will result in acceptable structural safety conditions of historic constructions.

In the present case, the first necessary action is to prevent the façade collapse mechanism previously mentioned (Fig. 1(c)). Such a condition could be attained by imposing block-like behavior on the building through a rigid diaphragm which connects the tops of the walls at the base of the roof. This is a possible intervention, because it would be hidden by the presence of the ceiling system and it could be realized by means a plane structure of steel braces, for example.

Two possible structural solutions are therefore considered (type A and type B). Both of them provide the presence of a rigid diaphragm that connects the tops of the masonry walls: in solution A, the rigid plane connects the tops of only the masonry walls enclosing the entrance area, while in solution B it connects the tops of all the masonry walls.

It is expected that, due to insufficient masonry strength and ductility, the conventional strengthening interventions describe above would improve the seismic response capacities of the building, but would not allow the building to reach an adequate safety level.

Please cite this article in press as: M. Pauletta, et al., Seismic rehabilitation of cultural heritage masonry buildings with unbonded fiber reinforced elastomeric isolators (U-FREIs) – A case of study, Journal of Cultural Heritage (2017), https://doi.org/10.1016/j.culher.2017.09.015

Strengthening of the masonry walls would entail invasive interventions, to give the structure the capacity to dissipate earthquake energy throughout the inelastic response of its elements, or to respond elastically to the design earthquake. This is why it was decided to use seismic isolation.

8. Base isolation for seismic rehabilitation

Differently from conventional types of retrofit interventions, the base seismic isolation technique decouples the structure from the horizontal components of the ground motion by interposing structural elements, the isolators, with low horizontal stiffness between the structure and the foundation, which are called super- and sub-structure, respectively. This layer gives the structure a fundamental frequency that is much lower than both fixed-base frequency and the predominant frequencies of the ground motion. The first dynamic mode of the isolated structure involves deformation only in the isolation system, the structure above being to all intents and purposes rigid [38].

The decrease in the fundamental frequency produces reduction of the acceleration acting on the structure. Further acceleration reduction is provided by the energy absorption capability of the devices. These bearings, which can be replaceable if such need arises, are placed between the building and its foundation,

Seismic isolation is usually used for new buildings, but it is also effective, when applicable, for seismic protection of existing buildings, in particular cultural heritage sites [39,40] or even for protection of art objects [41].

The applicability of isolation technique must be assessed with regard to two main aspects, namely: the absence of adjacent buildings or the feasibility of separating the isolated building from neighboring structures, and the possibility of removing the ground floor to create a working area for the installation of the isolators.

8.1. Proposed rehabilitation intervention

The retrofit action proposed herein involves the use of an innovative type of isolation device, the Unbonded Fiber-Reinforced Elastomeric Isolator (U-FREI), according to the method of production described in [42,43].

Studies on U-FREIs began at the end of the 1900s and at early 2000s with first publications of J.M. Kelly and co-workers at the Earthquake Engineering Research Center (University of California at Berkeley) [44–48], who started to study this innovative type of elastomeric bearings with the main aim of promoting the development of low-cost natural rubber isolation systems for the seismic protection of public housing in developing countries.

The fiber reinforced elastomeric bearings revealed to be valuable devices for seismic isolation of buildings, hence research on their utilization continued and spread during the years involving several research groups around the world. Theoretical [49–57] and experimental studies [58–65] also on shaking table [66], [67] were carried out, which allowed to satisfactorily understand U-FREIs behavior.

Analyses of buildings isolated by means of U-FREIs can also be found [68–70], however only one application [70] has been developed until now about the utilization of U-FREIs to isolate historical buildings.

U-FREIs, unlike the more commonly used Steel-Reinforced Elastomeric Isolators (SREIs), which are reinforced by steel plates, are reinforced by carbon fiber fabrics and do not need anchorages to the sub- and super-structures. U-FREIs' fabric reinforcements can be the same used for retrofit of existing structures [71,72] and can have fibers along two principal directions, at 0° and 90°, or along four directions at 0°, 45°, 90° and 135° [42,43]. The manufacturing cost of fiber reinforced isolators is greater than that of traditional ones, due to the major cost of the fibers. Anyhow, the costs connected with the labor involved in preparing the steel reinforcement (cutting, sandblasting, cleaning with acid, and coating with bonding compound) are eliminated. Moreover the absence of end-plates for the anchorage to the structure and the substitution of the steel reinforcements with fiber ones reduces the isolator's weight. Hence, being fiber-reinforced isolators much lighter than the traditional ones and also less voluminous, transportation and installation are simpler and the relevant costs are lower than those for traditional isolators. It results that the overall cost of a fiber-reinforced isolator is a little lower than a traditional one [62].

Being U-FREIs not anchored to the sub- and super-structure, the "absence of compression" causes the detachment between the super-structure and the device. This situation is not catastrophic for the isolator itself, because it remains unloaded. However, since the whole seismic action is borne by the other devices, which are still in contact with the superstructure, these devices have to be verified.

In a previous research work [73] the possibility of using isolation techniques for the Lippomano Villa Oratory was assessed, and a method for the installation of U-FREIs at the base of the church was developed.

The intervention begins with the removing of the indoor flooring. Then two excavations parallel to the foundation, one inside the building and the other outside, are realized in order to create an adequate working area for the installation of the devices. A double bottom ring of reinforced concrete, one internal and the other external, parallel and adjacent to the existing foundation, is realized in the excavations to create a new rigid sub-foundation. Then the masonry is cored with constant pitch along the entire perimeter of the building. The coring is performed below the ground level, thus preserving any internal or external precious plaster. Threaded steel rods are inserted in the holes to connect two steel elements, which are placed on both sides of the wall in order to jacket the masonry (Fig. 4(a)). Hydraulic jacks are installed between the steel beams and the foundation concrete rings to keep the structure in position during the cutting of the masonry. Then the masonry below the steel profiles is cut and removed, ashlar after ashlar, and the seismic devices are inserted into the cavity (Fig. 4(b)). Cross bracings of steel elements are installed inside the building, above the level of the isolators, to form a rigid horizontal plane [74].

It should be noted that the isolation plane is located above the foundation and below the ground level, hence it affects neither the aesthetic appearance of the building nor its artistic and historical heritage. Not even the moat surrounding the building impacts the architecture because it is covered at the ground level by an element, which bears the vertical loads but is deformable or slides under horizontal loads. A possible technical solution for this element is a stainless steel sheet adequately thick for vertical loads, connected by means of bolts to the existing structures and leaned on a sliding support anchored to the moat external retaining wall. The steel sheet must have an adequate width in order to cover the moat under the maximum design displacement of the isolation system.

The aim of seismic isolation is to produce an increase in the first mode period of the structure, with consequent reduction of the seismic acceleration. However the use of only U-FREIs did not lead to a sufficient high period for the considered structure, hence it was decided to reduce the number of isolators substituting some of them with Flat Surface Sliders (FSS). Since FSS devices have a negligible horizontal stiffness, the overall horizontal stiffness of the isolating system was in this way reduced and a satisfactory first mode of vibration period T_{is} was reached.

Both the U-FREIs and FSS bearings support vertical loads and allow the isolation plane to move laterally with relatively low lateral stiffness, the latter provided by the elastomeric devices. A hybrid base seismic isolation system, consisting in

Please cite this article in press as: M. Pauletta, et al., Seismic rehabilitation of cultural heritage masonry buildings with unbonded fiber reinforced elastomeric isolators (U-FREIs) – A case of study, Journal of Cultural Heritage (2017), https://doi.org/10.1016/j.culher.2017.09.015

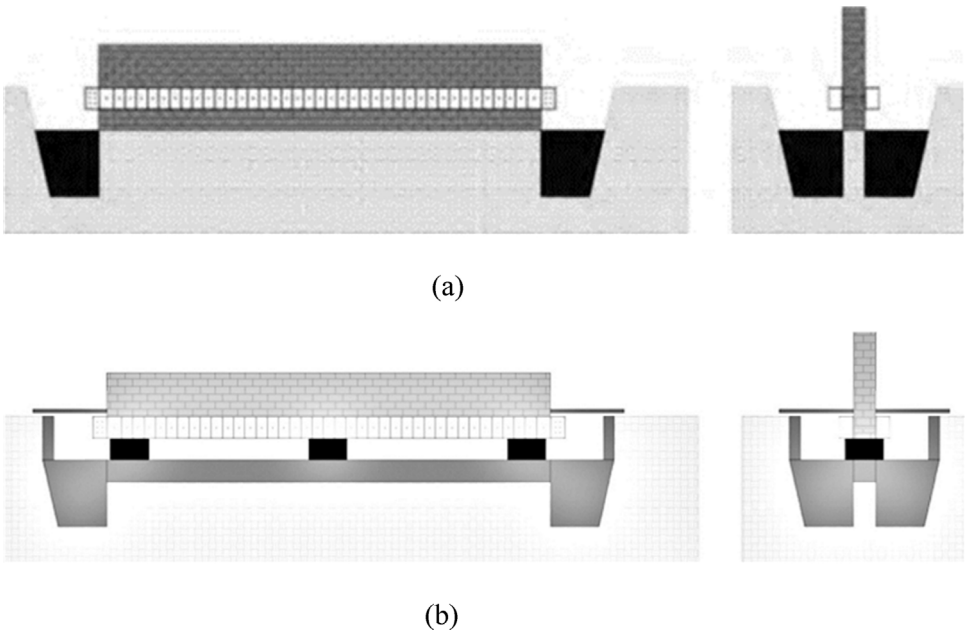

Fig. 4. (a) Jacketing of masonry with steel profiles; (b) cutting/removing of the masonry below the steel profiles and insertion of seismic devices into the new cavity [73].

six square-shaped U-FREI devices and six flat surface sliders is designed for the Lippomano Villa Oratory.

The location of the U-FREIs and FSS bearings is shown in Fig. 2(b). Their size is chosen on the basis of the maximum vertical acting load, which is 606.7 kN for FSS bearings and 473.9 kN for U-FREIs.

While properties of FSS bearings are provided by the manufacturer [75], U-FREIs are designed on the basis of previous experimental tests and studies performed on these devices [53,54,59,62]. Since these studies, which allow to derive the isolator constitutive relationship [57], regarded square shaped isolators, the devices designed herein have this shape.

Also a preliminary selection of SREIs is performed on the basis of the devices available in the market [75], to make a comparison in terms of size and isolation capacity between U-FREIs and SREIs.

Geometric characteristics of the selected devices are: square shape in plan with side length of 600 mm and height of 270 mm for U-FREIs, and circular shape in plan with diameter of 650 mm and total height of 313 mm for SREIs. From these device sizes it can be observed that the volume of the U-FREI is smaller (−6,4%) than that of the SREI.

Both devices are made with soft elastomeric compound having shear modulus equal to 0.4 MPa. The rubber layer thickness is 263 mm for U-FREIs and 207 for SREIs. The maximum allowed displacements are 450 mm and 400 mm for U-FREIs and SREIs, respectively. Other U-FREI characteristics are as follows: individual rubber layer thickness equal to 8 mm, fiber layer thickness 0.2 mm, primary shape factor = cross sectional area of rubber/free surface area of a single rubber layer = 18.8, and secondary shape factor = isolator side length/rubber total thickness = 2.3. The isolator bulk modulus can be assumed equal to 2000 MPa.

The type of adopted FSS device is a PTFE flat sliding support produced by IBG MONFORTS (Germany), model N 806 [76]. The device has square shaped plan with side length of 520 mm, height of 165 mm and vertical capacity of 1750 kN. The movement range of the support is equal to 460 mm, i.e. the allowed displacement is ± 230 mm. The coefficient of static friction is equal to 0.02. The FSS device is modeled with a non-liner behavior: it does not work if subjected to vertical tensile action, while it works if subjected to compression. For the compression condition, the authors assigned to the device a linear elastic behavior, neglecting its dissipative characteristics. The elastic modulus of this linear law is equal to 10^{-7} MPa.

To evaluate the effects of the seismic retrofit, dynamic time-history analyses are performed using SAP2000. The seismic isolators and the pre-existing anchoring ties (Fig. 1(b)) are the only elements having a non-linear behavior, hence the Fast Non-Linear Analysis (FNA) tool is used [37]. The aim of the analysis is to assess whether the stress state of the masonry remains within the elastic domain during the entire seismic event.

The vertical acceleration is not considered in the church analyses, because the isolator vertical stiffness (304680 N/mm) is adequately high, with respect to the horizontal one (497 N/mm in Table 1), to avoid rocking of the structure.

8.2. Modelling of U-FREIs

Each U-FREI device is modeled by assembling three finite elements in the following order: Friction Pendulum (NLLink), Hysteretic Rubber Isolator (NLLink), Friction Pendulum (NLLink).

Friction Pendulum elements transfer vertical and horizontal loads only when they are subjected to compressive stresses, while, in the presence of tensile vertical action, no load is transferred. The amount of transferred horizontal load depends on the value of the coefficient of static friction assigned to the element. Analogously, since U-FREIs are not anchored to sub- and super-structure, they transfer vertical and horizontal loads only when subjected to compressive stresses and the amount of transferred horizontal load depends on the friction conditions of the contact surfaces, i.e. material type of sub-and super-structure and roughness degree of the surfaces. On the basis of previous observations, the upper and lower Friction Pendulum of the proposed assembly allow to well represent the contact behavior between U-FREI and super- and sub-structure. The characteristics assigned to these elements are: flat sliding surface, to avoid uplift movements of the super-structure, and coefficient of static friction equal to 0.93, assumed on the basis of previous experimental tests [53] considering sub- and super-structure concrete contact surfaces. This value is high, because no slip is expected among the U-FREI and the sub- and super- structure if the isolator is subjected to compressive stresses.

Please cite this article in press as: M. Pauletta, et al., Seismic rehabilitation of cultural heritage masonry buildings with unbonded fiber reinforced elastomeric isolators (U-FREIs) – A case of study, Journal of Cultural Heritage (2017), https://doi.org/10.1016/j.culher.2017.09.015

Table 1
Parameters for analyses and verifications.

Type of device	Horizontal effective stiffness [N/mm]	Elastic stiffness [N/mm]	Post-yield stiffness [N/mm]	Yield strength [kN]	Characteristic strength [kN]	Maximum allowed displacement [mm]
U-FREI	497	2104	334	41.7	217	450
SREI	641	4209	422	53.8	186	400

The Hysteretic Rubber Isolator element allows to describe the hysteresis isolator behavior under horizontal loads. This is done using a simplified bi-linear constitutive relationship, which can be derived from experimental results, as explained in [57].

SREIs devices, being anchored to the super- and sub-structure, can be modeled using only the Hysteretic Rubber Isolator.

When linear analyses are performed, both U-FREI and SREI devices are modeled as linear elastic elements having stiffness equal to the horizontal effective stiffness specified in Table 1. For non-linear analyses a bi-linear relationships can be employed using the parameters reported in Table 1.

9. Seismic response of the structure

9.1. Existing condition seismic response

From the incremental dynamic analysis performed with ANSYS, it was observed that the building is not significantly damaged if the PGA value is less than or equal to 0.035 g. This acceleration corresponds to a return period of design ground motion TR of 16 years, a period much shorter than the return period relevant to the FDE, which is equal to 30 years (Fig. 5).

Since the church was built in the seventeenth century, it is statistically probable that a low intensity earthquake, corresponding to the return period greater than 16 years, has already occurred during the life of the building. This could explain the crack pattern visible on the south façade of the church before the renovation of the plaster (Fig. 1(a)) and, correspondingly, the cracks present inside the building, visible in section in Fig. 2(a).

In particular, non-linear dynamic analyses of the building under a seismic event having a PGA value of 0.309 g (MCE) predicts that, after 1 second, a failure mechanism involving the collapse of the upper middle part of the church south façade occurs.

Such a mechanism is immediately evident in Fig. 6(a), which shows the stress pattern provided by SAP2000 on the south façade at the time instant $t = 1.0$ s. The shell elements, which have a darker

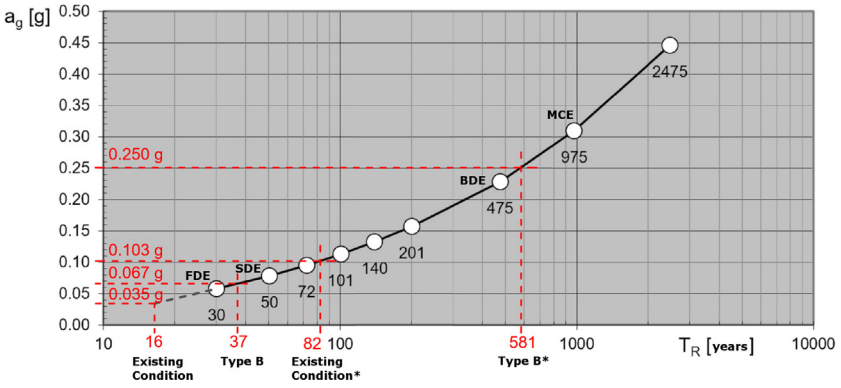

Fig. 5. Relationship between peak ground acceleration ag and return period of ground motions TR for the case study [77].

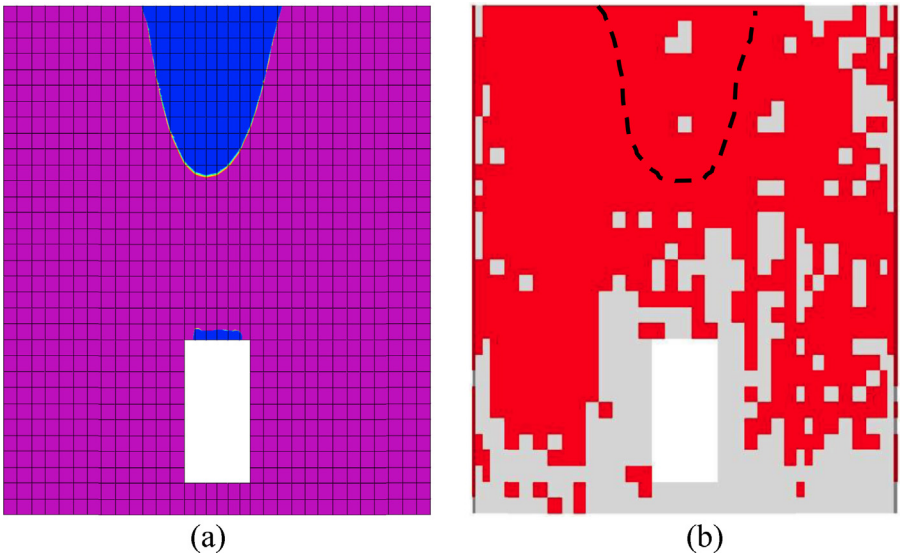

Fig. 6. South wall under the application of the MCE: (a) tensile stress map (SAP2000) at $t = 1$ s; and (b) crack pattern (ANSYS) at $t = 2$ s.

Please cite this article in press as: M. Pauletta, et al., Seismic rehabilitation of cultural heritage masonry buildings with unbonded fiber reinforced elastomeric isolators (U-FREIs) – A case of study, Journal of Cultural Heritage (2017), https://doi.org/10.1016/j.culher.2017.09.015

color in Fig. 6(a), are subjected to tensile stresses exceeding the masonry strength limit value of 0.1 MPa.

In the literature [36,37] it is reported that the damage of the masonry is visible on the surface of the wall only if the tensile stress limit for masonry is reached in at least two of the main directions of the element quadrature point. Fig. 6(b) shows in a darker color the only elements subjected to these conditions of stress at $t = 2.00$ s for the MCE. From this figure it can be observed that seismic acceleration peaks subsequent to that occurred at $t = 1$ s cause increased damage in the masonry wall. In particular the damage at $t = 2.00$ s is sufficiently extended to produce the disarticulation of the masonry and the possible incipient expulsion of its upper portion (schematically enclosed by the dashed line in Fig. 6(b)).

By referring to a seismic event having a PGA value of 0.035 g, the stress state occurring in the SAP2000 model in the interior wall is compatible with the beginning, at the middle of the door open, of the crack visible in Fig. 2(c). The result obtained by means of ANSYS is similar.

Both obtained results, however, are not sufficient to justify surface damage to the interior wall of the church. While, if the MCE with PGA of 0.309 g is applied to the structure, a vertical crack, like the one visible in Fig. 2(c), occurs at time $t = 2$ s. This means that the church has likely been subjected to an earthquake with a PGA greater than 0.035 g, which caused the formation of that crack.

To assess previous considerations a research on main earthquakes occurred in the area near the considered construction was carried out. It was found that historically there have been no major earthquakes in Monticella, but the potential of the fault (Montello fault) in whose influencing area the construction is located is $M_w = 6.7$ according to the moment magnitude scale [78].

From the Italian macrosesismic database, it can be found that six earthquakes having magnitude above four occurred in the past in the Montello fault influencing area, the highest of which in 1900 with $M_w = 5.13$.

Since the 1970s the instrumental seismicity of the area has been recorded by the Italian seismological research center [79], which has a network for locating shocks in the Northeast of Italy. Since 1977, 247 shocks have been recorded in the Montello fault influencing area, with a maximum magnitude of 4.0 in 1980.

Many ground motion equations exist for the prediction of earthquake peak ground acceleration on the basis of the magnitude, among which the one of Sabetta and Pugliese [80] is calibrated only on Italian accelerometers data. This equation is used herein to evaluate the PGA of the above mentioned earthquakes having magnitudes equal to 4 and 5.13.

$$\log a_{max} = -1.562 + 0.306 \cdot M_w - \log\left(r^2 + 5.8^2\right)^{0.5} + 0.169 \cdot S$$

Where r(km) = epicentral distance for earthquakes with $M_w \leq 6$; $S = 0$ for stiff soil sites and deep alluvial deposits (depth greater than 20 m) and $S = 1$ for superficial deposits (depth from 5 m to 20 m).

Considering that the average distance between Monticella and the Montello fault is around 12 km and that the village is located above deep alluvial deposits ($S = 0$), the resulting peak ground acceleration for $M_w = 4$ is $a_g = 0.034$ g, and for $M_w = 5.13$ is $a_g = 0.076$ g.

From these results it can be said that the church has certainly been subjected to an earthquake having at least a PGA equal to 0.034 g that is practically the value individuated as the one inducing the described crack pattern in the church south façade (Fig. 1(a)).

Fig. 7 shows the shear base reactions trend along the seismic force directions, which coincide with the main axes of the building (dir. 1: East-West and dir. 2: South-North).

The dotted line represents the response obtained from the linear analysis, the solid one the response of the non-linear analysis.

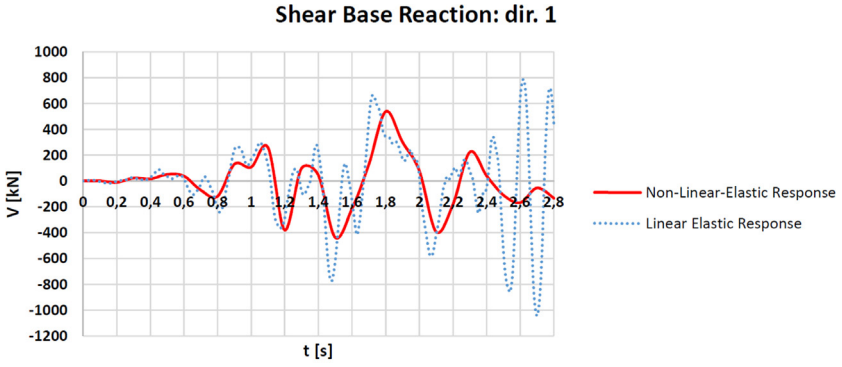

(a)

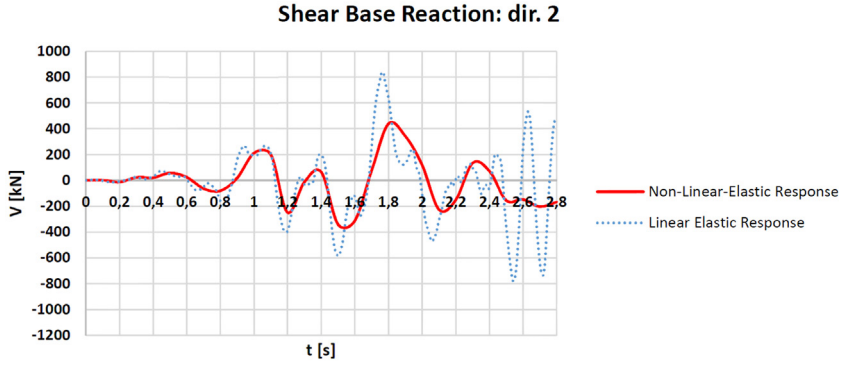

(b)

Fig. 7. Shear base reactions trend for the MCE: (a) east-west direction, (b) south-north direction.

Please cite this article in press as: M. Pauletta, et al., Seismic rehabilitation of cultural heritage masonry buildings with unbonded fiber reinforced elastomeric isolators (U-FREIs) – A case of study, Journal of Cultural Heritage (2017), https://doi.org/10.1016/j.culher.2017.09.015

Table 2
Key performance indicators for the two models.

	ANSYS	SAP2000
Modal analysis		
1st mode period [s]	0.34	0.36
1st mode participating mass ratio [%]	14.8	15.9
FNA at time equal to 1 s		
Damage	Cracking in the south façade upper part	Tensile stresses in the south façade upper part > masonry tensile strength
Shear base reaction in dir. 1 [kN]	100	120
Shear base reaction in dir. 2 [kN]	210	200

It is evident that the progressive damage of the masonry, taken into account by the non-linear model, modifies the response of the structure over time, in comparison with the linear response. At $t = 2.2$ s the two responses have few similarities in both the East-West and South-North directions, and the non-linear response of the damaged building becomes almost indifferent to the seismic input; this means that the numerical collapse condition has been reached.

The key performance indicators for the two models described above are summarized in Table 2.

9.2. Seismic response after traditional rehabilitation interventions

An estimate of the seismic safety level achieved by means each traditional rehabilitation intervention is obtained through incremental dynamic analyses performed on 3D models of the church subjected to the interventions.

Proceeding as previously described for the church in its present state, it was estimated that the church with the type A structural intervention may be damaged by earthquakes with PGA greater than 0.041 g, which corresponds to a return period of design ground motion equal to 19 years, a period shorter than the 30-year value provided for the Frequent Design Earthquake (FDE).

In the same way, it is estimated that the church with the type B structural intervention may be damaged by earthquakes with PGA greater than 0.067 g, which corresponds to a return period of design ground motion equal to 37 years, or 7 years longer than the value provided for FDE, but lower than the value provided for the Serviceability Design Earthquake (SDE), which is equal to 50 years (Fig. 5).

Fig. 8 shows the shear base reactions trend along the seismic force directions for the MCE.

The dotted line represents the response of the new structural configurations (type A in (a) and (c); type B in (b) and (d)), according to the linear analysis performed by means of SAP2000.

The dashed and the solid lines represent the behavior of the church in its existing condition and with the new structural configurations, respectively, according to the non-linear analysis performed by means of ANSYS.

From Fig. 8 it can be observed that masonry damage modifies the building structural response: it is evident that both the church in its present state and with the structural intervention A (Fig. 8(a) and (c)) becomes indifferent to the seismic input in both directions from the instant $t = 2.2$ s onwards. Hence, from this instant, the structure can be considered collapsed. This result demonstrates the ineffectiveness of intervention type A in improving the building behavior to cope with the design earthquake. Conversely, the greater value of the base shear reactions developed by the structure with the intervention type B (Fig. 8(b) and (d)) at the time instant of 2.2 s, shows that this structural configuration is still able to react to the seismic input, although the amplitude and frequency of the reactions are different from the elastic response (dotted line) due to the damage that has developed in the structure.

It can be concluded that the presence of the rigid diaphragm above all the masonry walls (intervention type B), allowing a better redistribution of the seismic forces among the walls, increases the resistance capacity of the building. However, at $t = 2.4$ s masonry crushing occurs at the side windows of the chapel.

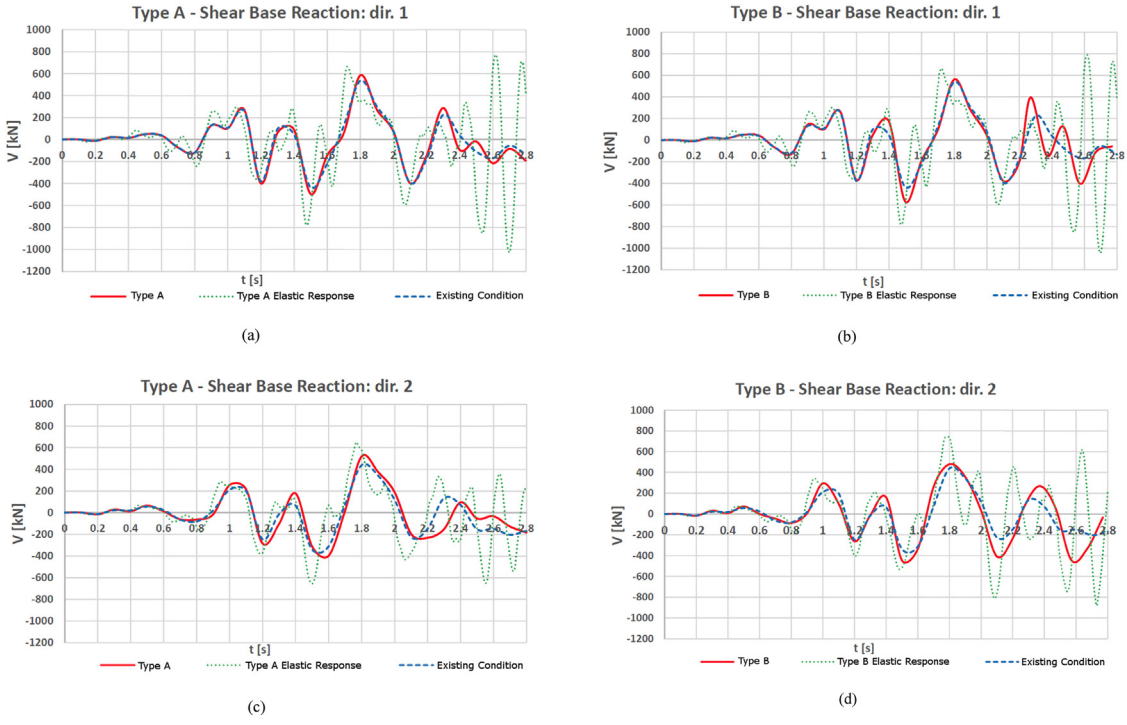

Fig. 8. Shear base reactions trend for the MCE. (a) and (b) east-west direction; (c) and (d) south-north direction.

Please cite this article in press as: M. Pauletta, et al., Seismic rehabilitation of cultural heritage masonry buildings with unbonded fiber reinforced elastomeric isolators (U-FREIs) – A case of study, Journal of Cultural Heritage (2017), https://doi.org/10.1016/j.culher.2017.09.015

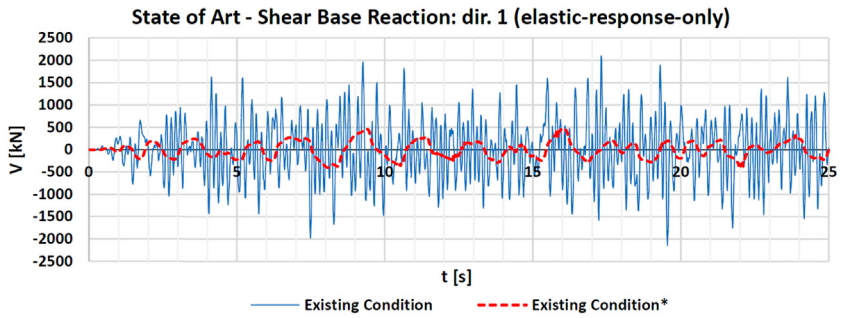

(a)

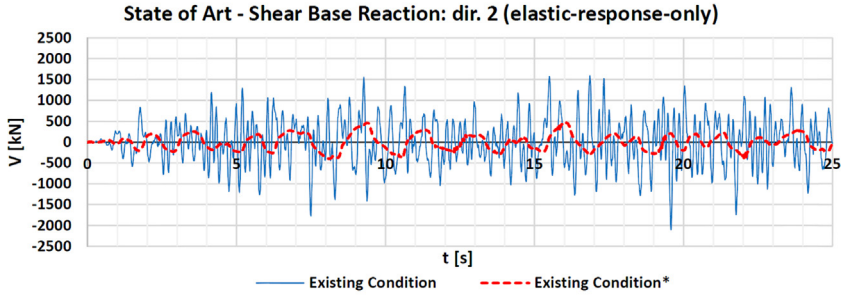

(b)

Fig. 9. Existing condition and existing condition* shear base reactions trend for MCE: (a) east-west direction, (b) south-north direction.

9.3. *Seismic response after the proposed intervention*

The efficiency of the designed seismic base isolation system is assessed considering the three structural configurations discussed above, i.e.: the church in its present state (existing condition), with intervention type A, and with intervention type B.

The behavior of the isolated structures is compared to the behavior of corresponding fixed base structures. To be distinguished from the corresponding fixed base structural configurations, the base isolated structural configurations are henceforth identified with asterisks, i.e.: existing condition*, type A* and type B*.

In order to compare the response of the U-FREI and SREI isolation systems, in terms of isolating period, displacement and base shear, equivalent static analyses are performed, assuming that the total horizontal effective stiffness of the isolating system is equal to the sum of the devices effective stiffness.

From these preliminary analyses it is estimated that:

- the vibration period is 2.2 s and 1.94 s for the church isolated by U-FREIs and SREIs, respectively, hence the vibration period is 13% higher in the first case;
- the maximum device displacement is equal to 193 mm for U-FREIs system and 170 mm for the SREIs system, respectively, hence the maximum displacement is 14% higher in the first case;
- the church isolated by means of U-FREIs achieves lower maximum base shear (−12%) than the church isolated by means of SREIs.

The observed results are due to the U-FREIs' lower effective horizontal stiffness.

On the whole it can be said that the U-FREIs' isolation capacity is better than the capacity of SREIs. Once it was determined that the U-FREI devices perform better than the SREIs, only the results of analyses relevant to the structure isolated by means of U-FREIs were considered.

In Fig. 9 the shear base reactions trends of the fixed base configurations are compared to the corresponding base isolated configurations for the MCE. Assuming linear-elastic-only behavior for masonry in both cases, the diagrams in Fig. 9 show that the designed seismic isolation system significantly lowers the highest stress peaks and decreases the oscillation frequency of the building in both main directions. Indeed the period of the base isolated structure derived from the modal analysis is 2.12 s for the existing condition* configuration and it is 2.23 for type B* configuration. Hence, considering the first period of vibration obtained by SAP2000 from the modal analysis of the structure for the Existing condition configuration (Table 2), the percentage increase of the period attained in presence of isolation is equal to 490%.

To make a comparison among the base shear acting on the structure in all the considered configurations, the corresponding maximum absolute shear values in both direction 1 and 2, V_1 and V_2, respectively, are reported in Table 3. The base shear reductions (ΔV_1 and ΔV_2) due to seismic isolation are reported for every configuration in the last two columns. As it can be seen from the data in the table, all isolated configurations provide a base shear reduction

Table 3
Maximum absolute shear values in direction 1 and 2 for all the considered configurations.

Fixed base structure				
		V_1[kN]		V_2[kN]
Existing condition		2149		2108
Type A		2137		1753
Type B		2139		2383
Isolated structure				
	V_1[kN]	V_2[kN]	ΔV_1[%]	ΔV_2[%]
Existing condition*	471	476	−78	−77
Type A*	480	485	−78	−72
Type B*	477	482	−78	−80

Please cite this article in press as: M. Pauletta, et al., Seismic rehabilitation of cultural heritage masonry buildings with unbonded fiber reinforced elastomeric isolators (U-FREIs) – A case of study, Journal of Cultural Heritage (2017), https://doi.org/10.1016/j.culher.2017.09.015

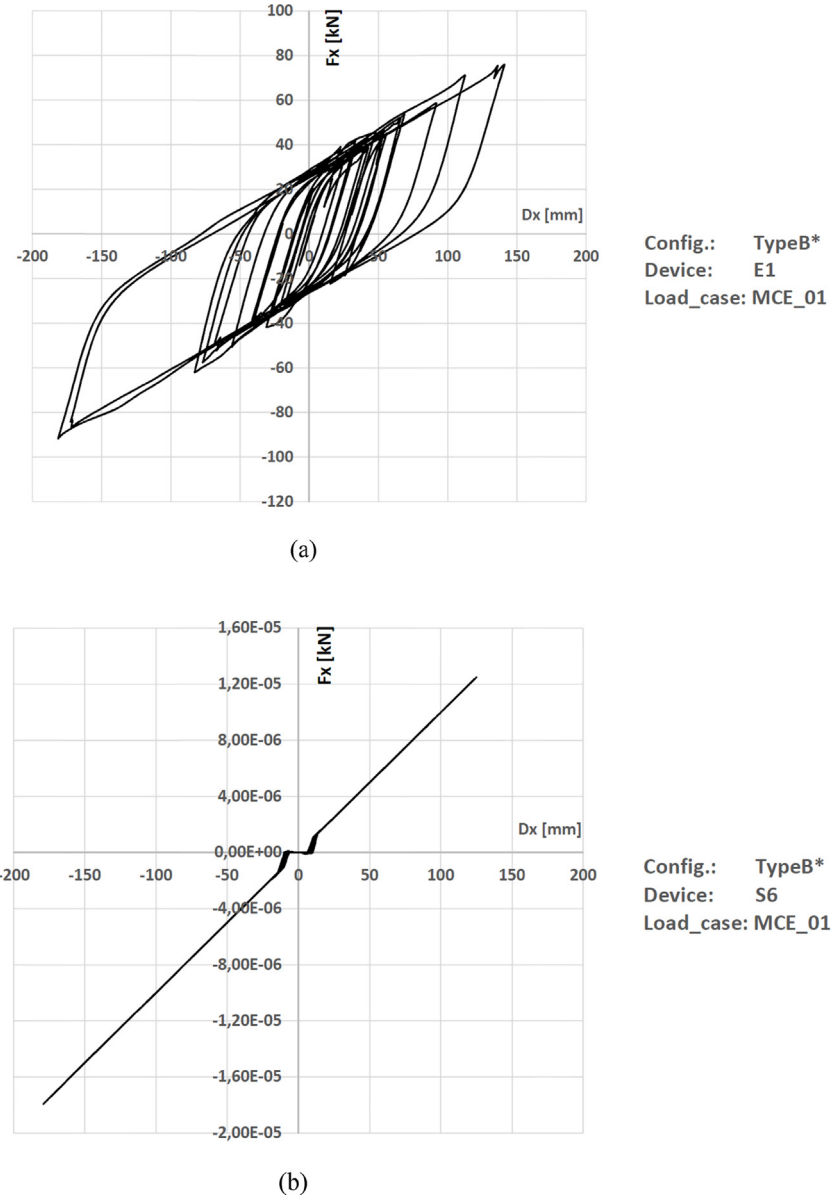

Fig. 10. Hysteresis loops under the MCE earthquake for the: (a) U-FREI E1, and (b) FSS.

of 78% in direction 1, while the maximum reduction in direction 2 (80%) is provided by configuration type B*.

Proceeding as described in sections 7 and 8 for the fixed-base structural configurations, through incremental dynamic analysis it is observed that the Existing Condition* structure is not significantly damaged if the PGA value of the seismic action is less than or equal to 0.103 g. This PGA corresponds to a return period of design ground motions of 82 years (Fig. 5), which is significantly longer than the TR value provided for SDE (50 years) and more than twice the value reached with the conventional intervention type B, for which TR = 37 years.

Under the MCE the U-FREIs subjected to the maximum lateral displacements D1 and D2 in the two main directions are the devices identified as E1 and E6 in Fig. 2(b), respectively. The calculated values of the maximum displacements are, respectively, D1 = 183 mm (E1 device) and D2 = 180 mm (E6 device). These displacements can be easily tolerated by the designed U-FREIs, which have a maximum allowed displacement of 450 mm. Displacements of this order of magnitude can be tolerated also by the FSS, which have a maximum allowed displacement of 230 mm.

However, after 3.6 seconds of analysis under the MCE, the stress state of the isolated church south wall is similar to that of the fixed base church after one second of the same analysis. Such a stress state implies an out-of-plane collapse mechanism.

On the basis of these results it can be said that base isolation alone is not so effective and the existing condition* isolated structure is still not able to resist very intense earthquakes, like the MCE, without collapsing. This occurs because, even after isolation, the church south façade remains slender and not effectively restrained to out of plane deformation at the top. Hence additional strengthening is required to the superstructure to further improve its behavior. In particular this result can be achieved only by restraining the church south façade at the top.

The goal is to achieve the elastic response of all the masonry walls for – at a minimum – the Basic Design Earthquake (BDE), which has TR = 475 years. To this end, in addition to the seismic isolation, the traditional interventions described in section 8 are taken under consideration. It is found that the isolated church with intervention type A (type A*) would be damaged by earthquakes with PGA greater than 0.182 g, which corresponds to a return period

Please cite this article in press as: M. Pauletta, et al., Seismic rehabilitation of cultural heritage masonry buildings with unbonded fiber reinforced elastomeric isolators (U-FREIs) – A case of study, Journal of Cultural Heritage (2017), https://doi.org/10.1016/j.culher.2017.09.015

Table 4
Acceleration peak values and return periods of the corresponding earthquakes that the structure can tolerate for all the scenarios.

Scenarios	Acceleration peak value [g]	Return period [years]
Existing condition	0.035	16
Type A	0.041	19
Type B	0.067	37
Existing condition*	0.103	82
Type A*	0.182	274
Type B*	0.250	581

of design ground motions equal to 274 years (Fig. 5). The isolated church with intervention type B (type B*) would be damaged by earthquakes with PGA greater than 0.250 g, which corresponds to a return period of 581 years (Fig. 5). Hence the type B* solution ensures the elastic response of all the masonry walls for seismic events of intensity greater than the one corresponding to BDE.

Regarding the behavior of the used devices, the hysteresis loops performed by U-FREI E1 and FSS S6 under the MCE earthquake are reported in Fig. 10(a) and (b), respectively. By comparing the two diagrams, it can be seen that the displacements are of the same order of magnitude, but not equal, because the two devices occupy different positions. Moreover the U-FREI performs elastic-hardening cycles and dissipates energy thanks to the viscous damping of rubber, while the FSS performs linear-elastic cycles as expected according to the linear elastic behavior assigned in compression.

No Slip is observed in the U-FREIs in any of the scenarios, because all the isolators are subjected to compression during the whole seismic action. Indeed the minimum observed compression under MCE is equal to 120.73 kN for isolator E1 (Fig. 9).

On the basis of the previous results, summarized in Table 4, it can be concluded that, by combining a seismic base isolation system, composed of U-FREI and FSS devices, and a rigid diaphragm connecting the tops of all the masonry walls, it is possible to achieve a high seismic performance level, i.e. a general elastic response of the structure for the Basic Design Earthquake (BDE).

10. Conclusions

On the basis of dynamic non-linear analyses performed on the Lippomano Villa Oratory, a masonry church of historical and artistic significance, subjected to earthquake loading, the following conclusions can be drawn:

- The structure in its existing condition is not able to ensure a general elastic response for a seismic event having intensity equal to that of the Frequent Design Earthquake (return period of 30 years);
- Earthquakes of intensity greater than the one having return period of 16 years could easily cause the formation of a mechanism that involves the collapse of the upper middle part of the church south façade;
- The two proposed reinforcing interventions of traditional type – intervention type A, with a diaphragm connecting the tops of only the masonry walls enclosing the entrance area, and intervention type B, with a diaphragm connecting the tops of all the masonry walls - are not effective in preventing the façade collapse mechanism under the Basic Design Earthquake (return period of 475 years), but allow only to bear earthquakes with return periods of 19 and 37 years, respectively;
- An advanced seismic retrofit solution is then proposed, consisting in the installation of six Unbonded Fiber-Reinforced Isolators (U-FREIs) and six Flat Surface Sliders (FSS);
- The building in the existing condition isolated configuration is not significantly damaged for seismic events with a return period up to 82 years;
- However, in order to achieve a general elastic response of all the masonry walls for the BDE, seismic isolation and reinforcing intervention type B should be used, allowing the church to remain elastic under an earthquake having a return period of 581 years > 475 years.

The approach described in the paper could be useful for the design of seismic protection interventions for other masonry cultural heritage buildings.

References

[1] M. Betti, A. Vignoli, Modelling and analysis of a Romanesque church under earthquake loading: assessment of seismic resistance, Eng. Struct. 30 (2008) 352–367.
[2] T. Choudhury, G. Milani, M. Acito, C. Chesi, C. Di Francesco, I. Carabellese, et al., 9th International Conference on structural analysis of historical construction, Damage survey and structural assessment of the Rosario Chruch in finale Emilia after the May 2012 earthquake in Emilia-Romagna Italy, SAHC2014, Emilia-Romagna, Italy, 2014.
[3] J. Heyman, The stone skeleton: structural engineering of masonry architecture, Cambridge University Press, Cambridge, UK, 1995.
[4] P.B. Lourenço, A matrix formulation for the elastoplastic homogenisation of layered materials, Mech. Cohesive-Frictional Mater. 1 (3) (1996) 273–294.
[5] V. Bosiljkov, Deliverable D9.0, in: Report on the state of the art on structural modelling of historical masonry structures, 2004.
[6] E. Sacco, A nonlinear homogenization procedure for periodic masonry, Eur. J. Mech. 28 (2009) 209–222 [A/Solids].
[7] P.B. Lourenço, G. Milani, A. Tralli, A. Zucchini, Analysis of masonry structures: review of and recent trends in homogenization techniques, Can. J. Civ. Eng. 34 (11) (2007) 1443–1457.
[8] R. Luciano, E. Sacco, Homogenisation technique and damage model for old masonry material, Int. J. Solids Struct. 34 (1997) 3191–3208.
[9] R. Luciano, E. Sacco, A damage model for masonry structures, Eur. J. Mech. A. Solids 17 (29) (1998) 285–303.
[10] L. Gambarotta, S. Lagomarsino, Damage models for the seismic response of brick masonry shear walls. Part I: the mortar joint model and its applications, Earthquake Eng. Struct. Dyn. 26 (4) (1997) 423–439.
[11] P.B. Lourenço, Anisotropic softening model for masonry plates and shells, J. Struct. Eng. N Y 126 (9) (2000) 1008–1016.
[12] C. Calderini, S. Lagomarsino, A micromechanical inelastic model for historical masonry, J. Earthquake Eng. 10 (4) (2006) 453–479.
[13] C. Calderini, S. Lagomarsino, Continuum model for inplane anisotropic inelastic behavior of masonry, J. Struct. Eng. 134 (2) (2008) 209–220.
[14] H.R. Lofti, P.B. Shing, Interface model applied to fracture of masonry structures, J. Struct. Eng. 120 (1) (1994) 63–80.
[15] P.B. Lourenço, J.G. Rots, Multisurface interface model for analysis of masonry structures, J. Eng. Mech. 123 (7) (1997) 660–668.
[16] G. Giambanco, S. Rizzo, R. Spallino, Numerical analysis of masonry structures via interface models, Comput. Methods Appl. Mech. Eng. 190 (2001) 3511–6493.
[17] F. Fouchal, F. Lebo, I. Titeux, Contribution to the modelling of interfaces in masonry construction, Construct. Build. Mater. 23 (2009) 2428–2441.
[18] R.C.G. Menin, L.M. Trautwein, T.N. Bittencourt, Smeared crack models for reinforced concrete beams by finite element method, Revista IBRACON Estrut. Mater. 2 (2) (2009) 166–200.
[19] M. Betti, L. Galano, Seismic analysis of historic masonry buildings: the vicarious palace in Pescia (Italy), Buildings 2 (2012) 63–82.
[20] S. Sorace, G. Terenzi, Analisi sismica di edifici storici in muratura mediante modelli globalmente non lineari, in: Workshop on design for rehabilitation of masonry structures, Edizioni Polistampa, Firenze, 2011, pp. 302–313.
[21] A.K. Moussalli, Isolamento sismico alla base per edifice esistenti d'interesse storico, architettonico e culturale–Innovative applicazioni strutturali con materiali avanzati, in: Ph. D. Thesis, University of Udine, Italy, 2014 [286 pp. in Italian].
[22] DPCM, Direttiva del Presidente del Consiglio dei Ministri 09.02.2011 per la valutazione e la riduzione del rischio sismico del patrimonio culturale con riferimento alle norme tecniche per le costruzioni DM 14.01.2008 GU no. 47 26. 02. 2011; 2011, 2011 [in Italian].
[23] E. Mele, A. De Luca, Behavior and modelling of masonry church buildings in seismic regions, in: Proceedings second international symposium on earthquake resistant engineering structures, 1999.
[24] P. Ronca, L. Castiglioni, Lo strumento dell'analisi numerica nelle fasi di diagnosi e di scelte progettuali per il consolidamento conservative di vecchie strutture. Atti IV Consegno ASSI.R.CCO, 1997, pp. 591–601 [in Italian].
[25] F. Genna, M. Di Pasqua, M. Veroli, Numerical analysis comparison models buildings: a constitutive of old masonry among constitutive models, Eng. Struct. 20 (1998) 37–53.

Please cite this article in press as: M. Pauletta, et al., Seismic rehabilitation of cultural heritage masonry buildings with unbonded fiber reinforced elastomeric isolators (U-FREIs) – A case of study, Journal of Cultural Heritage (2017), https://doi.org/10.1016/j.culher.2017.09.015

[26] Facchini L, Betti M, Biagini P, Vignoli A. RBF – Galerkin approach for the dynamics of simple disordered masonry structures. In: Atti XVII Congresso Nazionale AIMETA di Meccanica Teorica ed Applicata. 2005 [in Italian].
[27] Betti M, Orlando M, Vignoli A. Modelling and analysis of an Italian medieval castle under earthquake loading: diagnosis and strengthening. In: Proceedings of VI international conference on structural analysis of historical constructions. 2006 p. 1529-36.
[28] A. Grimaldi, R. Luciano, E. Sacco, Non-linear dynamic analysis of masonry structures via FEM, in: Computing methods in applied sciences and engineering, 1992, pp. 373–382 [Nova Science Publishers].
[29] E. Wilson, Three dimensional static and dynamic analysis of structures, CSI Inc, Berkeley, 1995.
[30] CSI, Analysis reference manual, 2016 [Computer and Structures, Inc.].
[31] ANSYS., Mechanical APDL element reference, 2013 [ANSYS Inc.].
[32] D. Drucker, W. Prager, Soil mechanics and plastic analysis or limit design, Q. Appl. Math. 10 (2) (1952) 157–165.
[33] K. Willam, E. Warnke, Constitutive model for the triaxial behavior of concrete Proceedings of the international Association for Bridges and Structural Engineering, 19, 1975, pp. 1–30.
[34] ANSYS, Mechanical APDL Theory Reference, 2013 [ANSYS Inc.].
[35] Ministero delle Infrastrutture, DM 14 gennaio 2008. Norme tecniche per le costruzioni, 2008 [in italian].
[36] S. Sorace, G. Terenzi, Analisi sismica di edifici storici in muratura mediante modelli globalmente non lineari. Workshop in design for rehabilitation of masonry structures, Edizioni Polistampa, Firenze, 2011, pp. 302–313 [in Italian].
[37] E. Petri, Modellazione mediante elementi finiti a fratturazione diffusa di un edificio storico in muratura. Thesis, University of Udine, Italy, 2011.
[38] J.M. Kelly, Earthquake-resistant design with rubber, Second edition, Springer-Verlag, London, 1997.
[39] E. Elsesser, M. Jokerst, S. Naaseh, Historic upgrades in San Francisco, Civil engineering, ASCE 67 (10) (1997) 50–53.
[40] S. Sorace, G. Terenzi, Analysis and seismic isolation of an older reinforced concrete vaulted building, Contemporary Eng. Sci. 9 (25) (2016) 1201–1215.
[41] S. Sorace, G. Terenzi, C. Bitossi, E. Mori, Mutual seismic assessment and isolation of different art objects, Soil. Dyn. Earthquake Eng. 85 (2016) 91–102.
[42] G. Russo, P. Angeli, I. Pitacco, M. Pauletta, A. Paschini, Seismic isolator and method to produce said seismic isolator. PCT/EP08/51779, 2010 [University of Udine].
[43] P. Angeli, A. Paschini, I. Pitacco, M. Pauletta, G. Russo, Brevetto di Isolatore Sismico e Procedimento per Realizzare Tale Isolatore Sismico, 2007 [0001380496, Università degli Studi di Udine].
[44] W. Taniwangsa, P.W. Clark, J.M. Kelly, Natural rubber isolation systems for earthquake protection of low-cost buildings, in: Report no. UCB7EERC-95/12, Earthquake Engineering Research Center, University of California, Berkeley, 1996.
[45] W. Taniwangsa, J.M. Kelly, Experimental and analytical studies of base isolation applications for low-cost housing, in: Report no. UCB7EERC-96/04, Earthquake Engineering Research Center, University of California, Berkeley, 1996.
[46] H.C. Tsai, J.M. Kelly, Stiffness analysis of fiber-reinforced elastomeric isolators. Report PEER 2001/05, Pacific Earthquake Engineering Research Center, University of California, Berkeley, 2001.
[47] S.M. Takhirov, J.M. Kelly, Analytical and experimental study of fiber reinforced elastomeric isolators. Report PEER 2001/11, Pacific Earthquake Engineering Research Center, University of California, Berkeley, 2001.
[48] J.M. Kelly, S.M. Takhirov, Analytical and experimental study of fiber reinforced strip isolators. Report PEER 2002/11, Pacific Earthquake Engineering Research Center, University of California, Berkeley, 2002.
[49] J.M. Kelly, Analysis of the run-in effect in fiber-reinforced isolators under vertical load, J. Mech. Mater. Struct. 3 (7) (2008) 1383–1401.
[50] S. Jiang, J. Hou, Y. He, Y. Yao, Mechanical study of fiber reinforced elastomeric isolator, China Civ. Eng. J. 45 (1) (2012) 227–232.
[51] P.M. Osgooei, M.J. Tait, D. Konstantinidis, Three-dimensional finite element analysis of square fiber-reinforced elastomeric isolators (FREIs) under lateral loads, Proceedings, in: Annual Conference, 2013, pp. 3074–3083 [Canadian Society for Civil Engineering].
[52] J.M. Kelly, A. Calabrese, Analysis of fiber-reinforced elastomeric isolators including stretching of reinforcement and compressibility of elastomer, Inge. Sismic. 30 (3) (2013) 5–16.
[53] G. Russo, M. Pauletta, Sliding instability of fiber-reinforced elastomeric isolators in unbonded applications, Eng. Struct. 48 (2013) 70–80.
[54] M. Pauletta, A. Cortesia, G. Russo, Roll-out instability of small size fiber-reinforced elastomeric isolators in unbonded applications, Eng. Struct. 102 (2015) 358–368.
[55] S. Pinarbasi, Y. Mengi, Analysis of fiber-reinforced elastomeric isolators under pure "warping", Struct. Eng. Mech. 61 (1) (2017) 31–47.
[56] N.C. Van Engelen, D. Konstantinidis, M.J. Tait, Simplified approximations for critical design parameters of rectangular fiber-reinforced elastomeric isolators, J. Eng. Mech. 143 (8) (2017) [art. no. 06017009].
[57] M. Pauletta, A. Cortesia, I. Pitacco, G. Russo, A new bi-linear constitutive shear relationship for Unbonded Fiber-Reinforced Elastomeric Isolators (U-FREIs), Compos. Struct. 168 (2017) 725–738.
[58] H. Toopchi-Nezhad, M.J. Tait, R.G. Drysdale, Testing and modeling of square carbon fiber-reinforced elastomeric seismic isolators, Struct. Control Health Monit. 15 (6) (2008) 876–900.
[59] G. Russo, M. Pauletta, A. Cortesia, A. Dal Bianco, Experimental behavior of carbon fiber reinforced isolators Santini A e Moraci N, 2008 Seismic engineering international conference commemorating the 1908 Messina and Reggio Calabria Earthquake, 1020, Reggio Calabria and Messina, Italy, 2008, pp. 1467–1474 [American Institute of Physics, Melville-New York. ISBN: 9780735405424].
[60] M.G.P. De Raaf, M.J. Tait, H. Toopchi-Nezhad, Stability of fiber-reinforced elastomeric bearings in an unbonded application, J. Compos. Mater. 45 (18) (2011) 1873–1884.
[61] H. Toopchi-Nezhad, M.J. Tait, R.G. Drysdale, Lateral response evaluation of fiber-reinforced neoprene seismic isolators utilized in an unbonded application, J. Struct. Eng. 134 (10) (2008) 1627–1637.
[62] G. Russo, M. Pauletta, A. Cortesia, A study on experimental shear behavior of fiber-reinforced elastomeric isolators with various fiber layouts, elastomers and aging conditions, Eng. Struct. 52 (2013) 422–433.
[63] E. Apostolidi, K. Bergmeister, A. Strauss, S. Dritsos, Experimental investigation on fibre reinforced elastomeric bearings, Eng. Prog. Nat. People (2014) 2478–2484.
[64] F. Hedayati Dezfuli, M. Shahria Alam, Performance of carbon fiber-reinforced elastomeric isolators manufactured in a simplified process: experimental investigations, Struct. Control Health Monit. 21 (11) (2014) 1347–1359.
[65] A. Calabrese, G. Serino, S. Strano, M. Terzo, Experimental investigation of a low-cost elastomeric anti-seismic device using recycled rubber, Meccanica 50 (9) (2015) 2201–2218.
[66] H. Toopchi-Nezhad, M.J. Tait, R.G. Drysdale, Shake table study on an ordinary low-rise building seismically isolated with SU-FREIs (stable unbonded-fiber reinforced elastomeric isolators), Earthquake Eng. Struct. Dyn. 38 (11) (2009) 1335–1357.
[67] A. Das, S.K. Deb, A. Dutta, Shake table testing of un-reinforced brick masonry building test model isolated by U-FREI, Earthquake Eng. Struct. Dyn. 45 (2) (2016) 253–272.
[68] H. Toopchi-Nezhad, M.J. Tait, R.G. Drysdale, Base isolation of small low-rise buildings using fiber reinforced elastomeric bearings Proceedings, annual conference - Canadian Society for Civil Engineering, 1, 2007, pp. 473–483.
[69] N.C. Van Engelen, D. Konstantinidis, M.J. Tait, Structural and nonstructural performance of a seismically isolated building using stable unbonded fiber-reinforced elastomeric isolators, Earthquake Eng. Struct. Dyn. 45 (3) (2016) 421–439.
[70] A. Castellano, P. Foti, A. Fraddosio, S. Marzano, G. Mininno, M.D. Piccioni, Seismic response of a historic masonry construction isolated by stable unbonded fiber-reinforced elastomeric isolators (SU-FREI), Key. Eng. Mater. 628 (2014) 160–167.
[71] G. Russo, M. Pauletta, Seismic behavior of exterior beam-column connections with plain bars and effects of upgrade, ACI. Struct. J. 109 (2) (2012) 225–233.
[72] G. Russo, O. Bergamo, L. Damiani, Retrofit with FRP elements and seismic performance assessment of the historic "castagnara" bridge in Padua, Italy, in: 34th International symposium on bridge and structural engineering: large structures and infrastructures for environmentally constrained and urbanised areas, 2010, pp. 554–555 [Venice, Italy].
[73] A. Moussali, M. Pauletta, D. Di Luca, Restauro sismico conservativo. Storia, tecnica e sostenibilità economica dell'isolamento sismico alla base Scienza e Beni Culturali, XXX, 2014, pp. 469–480.
[74] G. Russo, M. Pauletta, N. Scibilia, Long term structural deficiencies of a mat foundation on clay soil, J. Perform. Constructed Facilities 27 (3) (2013) 295–302.
[75] FIP Industriale anti-seismic devices (catalog).
[76] http://www.glt.ibg-monforts.de/katalog/katalog.pdf/katalog.pdf.
[77] Consiglio Superiore dei Lavori Pubblici. Spettri di risposta ver. 1.03.
[78] M.E. Poli, P. Burrato, F. Galadini, A. Zanferrari, Seismogenic sources responsible for destructive earthquakes in north-eastern Italy, Bull. Geophys. Theory. Appl. 49 (3–4) (2008) 301–313.
[79] http://www.crs.inogs.it/.
[80] F. Sabetta, A. Pugliese, Estimation of response spectra and simulation of nonstationary earthquake ground motions, Bull. Seismol. Soc. Am. 86 (1996) 337–352.

Please cite this article in press as: M. Pauletta, et al., Seismic rehabilitation of cultural heritage masonry buildings with unbonded fiber reinforced elastomeric isolators (U-FREIs) – A case of study, Journal of Cultural Heritage (2017), https://doi.org/10.1016/j.culher.2017.09.015